THE JOURNAL OF PHYSICAL CHEMISTRY Letters

Letter

pubs.acs.org/JPCL

On the Controversial Nature of the 825 nm Exciton Band in the FMO Protein Complex

Adam Kell,[†] Khem Acharya,[†] Valter Zazubovich,[§] and Ryszard Jankowiak*[,†,‡]

[†]Department of Chemistry and [‡]Department of Physics, Kansas State University, Manhattan, Kansas 66506, United States

[§]Department of Physics, Concordia University, Montreal H4B 1R6, Quebec, Canada

ABSTRACT: The nature of the low-energy 825 nm band of the Fenna–Matthews–Olson (FMO) protein complex from *Chlorobaculum tepidum* at 5 K is discussed. It is shown, using hole-burning (HB) spectroscopy and excitonic calculations, that the 825 nm absorption band of the FMO trimer cannot be explained by a single electronic transition or overlap of electronic transitions of noninteracting pigments. To explain the shape of emission and nonresonant HB spectra, downward uncorrelated excitation energy transfer (EET) between trimer subunits should be taken into account. Modeling studies reveal the presence of three sub-bands within the 825 nm band, in agreement with nonresonant HB and emission spectra. We argue that after light induced coherences vanish, uncorrelated EET between the lowest exciton levels of each monomer takes place. HB induced spectral shifts provide a new insight on the energy landscape of the FMO protein.

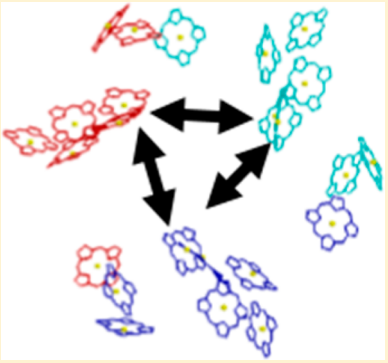

SECTION: Spectroscopy, Photochemistry, and Excited States

The Fenna–Matthews–Olson (FMO) protein of green sulfur bacteria is a long studied pigment–protein complex which funnels energy from the chlorosome to the reaction center.[1−3] This complex continues to be of great interest due to observed quantum effects, which were suggested to be responsible for the very high efficiency of excitation energy transfer (EET) in photosynthetic antenna complexes.[4,5] Until recently it was believed that each monomer of the FMO trimer binds seven bacteriochlorophyll *a* (BChl *a*) molecules. Recently X-ray diffraction and mass spectrometry data have confirmed the presence of an additional pigment (BChl *a* 8) located at the monomer connection regions with partial occupancy.[6−8] While there are multiple assignments of pigment site energies in the literature, it is well accepted that BChl *a* 3 and 4 contribute mostly to the lowest excitonic state in each monomer.[9−12]

There is a remarkable amount of experimental and theoretical papers related to the topic of excitonic structure of FMO, its vibrational environment, and the origin of measured[4,5] and simulated[10,13−16] long-lived quantum coherences. However, usually only the monomer is taken into account in simulations of excitonic structure,[17] energy transfer pathways,[18−21] and non-Markovian noise correlation effects.[22] This is in spite of a number of previously published experimental data obtained by hole-burning (HB) spectroscopy,[23,24] difference fluorescence line-narrowing (ΔFLN),[25,26] pump–probe spectroscopy,[27−29] photon echo experiments[30] and triplet minus singlet measurements,[31] as well as theoretical modeling,[32] which all suggested the possibility of intermonomer energy transfer in FMO proteins. Additionally, a very recent study considered three identical site distribution functions (SDFs) for the 825 nm band. In this simple model, it was assumed that the three states are localized on BChl *a* 3 only. The results also suggested that EET should be taken into account to explain the shapes of both resonant and nonresonant HB spectra.[33] In this work, using a model that incorporates excitonic interactions, we further challenge the present consensus[3,17] that the low-energy 825 nm band can be properly described by a single excitonic state. We focus on the nature of the lowest energy absorption band of FMO complexes from *Chlorobaculum (C.) tepidum*, which remains controversial.

The above-mentioned consensus is due to the fact that most authors in recent years have argued that the intersubunit coupling between BChl *a* 3 is too weak to warrant consideration for the entire trimer. However, Förster theory[34,35] predicts that energy transfer on the order of picoseconds is possible even for very weak ($|V| < 5$ cm^{-1}) electronic coupling between chromophores. The coupling constant between BChl *a* 3 and 4 (the lowest energy pigments within a monomer) is −53.5 cm^{-1}, when calculated from the crystal structure (PDB ID: 3ENI)[7] using the TrEsp method[36] and assuming a Q_y transition dipole strength of 25.2 D^2. (Effective dipole strength includes the influence of the dielectric constant). In this case the coupling between BChl *a* 3 pigments and BChl *a* 4 pigments located in various monomers is −2.5 and 2.5 cm^{-1}, respectively. It has been previously proposed that the three bands underlying the 825 nm absorption band may correspond to three transitions shifted by 20 cm^{-1}.[37] This model has not been accepted, as one would have to assume

Received: January 18, 2014
Accepted: April 1, 2014
Published: April 1, 2014

   dx.doi.org/10.1021/jz5001165 | *J. Phys. Chem. Lett.* 2014, 5, 1450−1456

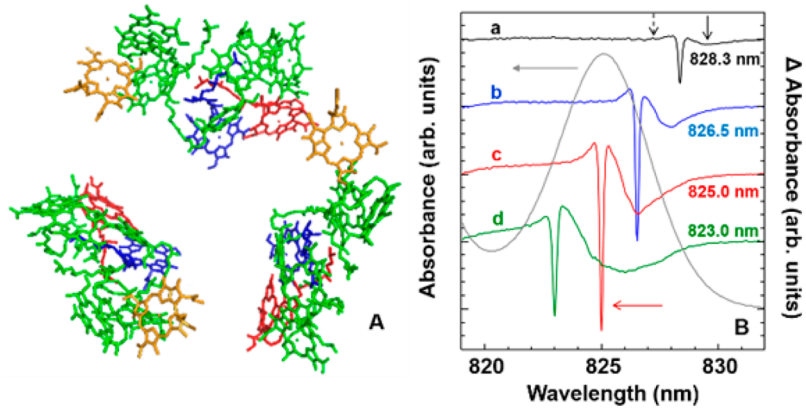

Figure 1. Frame A: Structure of the FMO trimer showing the orientation of BChl *a* pigments. BChl *a* 3, 4, and 8 are colored blue, red, and orange, respectively. Frame B: Resonant HB spectra burned within the 825 nm band. Spectra a–d were obtained with λ_B = 828.3, 826.5, 825.0, and 823.0 nm, respectively, and are shifted for clarity. The dashed and solid arrows mark the real- and pseudo-PSBHs, respectively, while the red arrow indicates (as an example) the intense ZPH for curve c. The gray curve is the absorption band.

different site energies for each monomer, an unlikely scenario. In addition, the Monte Carlo simulations did not provide downward EET rates consistent with the resonant HB spectra.[37] In contrast, we propose that the average site energies of BChls in each monomer are the same, but disorder causes the energies to vary between the three monomers of the trimer.

Figure 1 shows the 825 nm absorption band (gray curve) and four resonant (nonphotochemical) HB spectra obtained for burn wavelengths (λ_B) of 828.3, 826.5, 825.0, and 823.0 nm, curves a–d, respectively. All holes were obtained with a fluence (f) of 120 J cm^{-2}; the percent hole depths of curves a–d are 65.0%, 66.7%, 59.5%, and 47.4%, respectively. Although the resolution of these resonant holes is 1 cm^{-1}, we purposely burned deeper holes to demonstrate the presence of EET between subunits. Therefore, the widths of our zero-phonon holes (ZPHs) are power broadened. However, high-resolution (shallow) holes (using low fluence; hole depth <10%) were reported elsewhere, where the estimated lifetimes of the Q_y-states also indicated downward EET.[23,24] The shapes of the entire HB spectra in Figure 1 (curves a–d) also indicate the presence of downward energy transfer between FMO monomers. That is, low-energy satellite hole features are significantly more enhanced than would be warranted if EET was not present.

The narrow deepest holes are the resonant ZPHs coincident with λ_B, with pseudo- and real-phonon sideband holes (PSBHs) located ∼22 cm^{-1} to the red and the blue, respectively. A similar phonon frequency of 22 cm^{-1} was observed by Matsuzaki et al.[24] in FMO complexes from *Prosthecochloris (P.) aestuarii*. The spectra in Figure 1 clearly establish the existence of EET in that the bleaching to the lower energies with respect to the ZPHs is indicative of energy acceptors, not purely the pseudo-PSBHs as would be expected if the band was composed of a single exciton state. Thus, the pseudo-PSBHs are not well resolved in spectra b–d due to a broad contribution from downward EET, as pigments in different sub-SDFs, as discussed below, are burned due to direct transfer from the highest energy pigment subpopulation to the lowest energy subpopulation. That is, assuming the 825 nm band is composed of a single exciton state (no intraband EET and weak electron–phonon (el–ph) coupling), the pseudo-PSBH of curve d would be much narrower. Thus, our data indicates the presence of intermonomer EET. Therefore, in contrast to ref 37, where it was assumed that the 825 nm band is contributed to by three equi-spaced states (20 cm^{-1}) with widths of 50 cm^{-1}, we propose a model with identical SDFs for each monomer (*not* equi-spaced sub-bands) in which downward energy transfer between identical trimer subunits is taken into account.

More specifically, we suggest that not only the whole trimer has to be considered in simulations of optical spectra, but the presence of uncorrelated EET between the FMO monomers must be considered to explain both resonant and nonresonant HB spectra. Due to disorder and EET between BChl *a* 3 pigments (and in part BChl *a* 4 molecules, which have a small probability be the lowest energy pigments) in the three monomers, one sub-band of the 825 nm band should correspond to the lowest energy pigments in the trimer (that cannot transfer energy), with the second sub-band (shifted blue) corresponding to pigments that serve as an acceptor and donor, and the last sub-band corresponding to the highest energy pigments that efficiently transfer energy to the two lower energy acceptors (the two lowest energy subpopulations of BChls) within the trimer. Throughout this work we refer to these sub-bands (and pigments contributing to them) as sub-bands 1, 2 and 3; with band 1 being lowest in energy and band 3 being highest in energy. Thus, we assume that due to uncorrelated EET between subunits, the excitation energy can be transferred to either one of the energy acceptors and the process is competitive. This, as mentioned above, should lead to three *sub*-SDFs within the 825 nm absorption band, as illustrated below.

Regarding HB, pigments in resonance with narrow-band laser excitation may undergo a reaction (photochemical HB, PHB) or experience rearrangement of the local environment (nonphotochemical HB, NPHB).[38,39] These changes are reflected in HB spectra, which are the difference between absorption spectra measured before and after laser excitation. The resulting holes are persistent, meaning the holes are only removed by raising the temperature of the sample. For nonresonant HB, persistent holes are formed after energy relaxation to the lowest exciton states and the holes reflect the shape of the emitting state. Thus, in FMO, the pigments contributing to sub-band 1 will be burned first, as HB yield depends on the excited state lifetime. However, a partial bleaching of sub-band 2 cannot be entirely excluded. That is,

dx.doi.org/10.1021/jz5001165 | *J. Phys. Chem. Lett.* 2014, 5, 1450–1456

Table 1. Hamiltonian for Reduced Structural Model of FMO from *C. tepidum*

BChl *a*	3A	4A	3B	4B	3C	4C
3A	12 155	−53.5	−2.5	5.7	−2.5	0.5
4A	−53.5	12 245	0.5	2.5	5.7	2.5
3B	−2.5	0.5	12 155	−53.5	−2.5	5.7
4B	5.7	2.5	−53.5	12 245	0.5	2.5
3C	−2.5	5.7	−2.5	0.5	12 155	−53.5
4C	0.5	2.5	5.7	2.5	−53.5	12 245

Site energies and dipole coupling matrix elements are in units of cm^{-1}. BChl *a* 3 and 4 pigments from different monomers are designated as A, B, and C.

some bleaching of higher-energy pigments occurs because their HB yield is small but not zero; and once some sub-band 1 pigments experience NPHB, pigments that used to contribute to sub-band 2 become lowest-energy, and their HB yield increases.

In modeling of absorption, emission, and HB spectra, we assume that the lowest states of all three monomers have the same SDFs. To fit the 825 nm exciton band, emission band and low-energy hole, a reduced structural model is used (i.e., a trimer of BChl *a* 3 and 4 pigments) as, based on our calculations for the entire trimer (to be reported elsewhere) and literature data,[9−12] BChl *a* 3 mostly contributes to the lowest energy exciton with minor contributions from BChl *a* 4. Our excitonic modeling studies of various optical spectra revealed that the site energies for BChl *a* 3 and 4 are 12155 and 12245 cm^{-1}, respectively; with an inhomogeneous broadening (fwhm) of 90 cm^{-1}. The site energies apply to the structural model used in this work, as the site energy for BChl *a* 4 may change slightly when interactions with other pigments are included. The Hamiltonian used for the reduced structural trimer model of FMO is shown in Table 1. BChl *a* 3 and 4 pigments from different monomers are designated as A, B, and C. For monomer calculations (i.e., no intermonomer EET present; see Figure 2B), in order to fit the 825 nm absorption band the site energies of both pigments were red-shifted by 5 cm^{-1}. The solid (black) spectra in Figure 2 correspond to the experimental absorption, emission and the persistent nonresonant HB spectra, all obtained for *C. tepidum*. The corresponding noisy red (frame A) and blue (frame B) curves are the calculated spectra with and without EET between monomer subunits, respectively. Intramonomer interactions were modeled using Redfield theory,[40,41] with Förster energy transfer occurring between lowest energy molecules of various monomers.

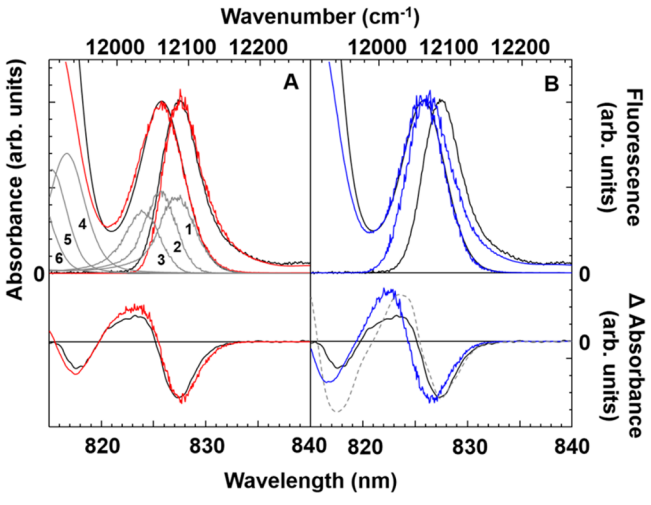

Figure 2. Frame A: Calculated (red) absorption, emission and HB (λ_B = 496.5 nm; f = 468 J cm^{-2}; hole depth at 827 nm = 3.6%) spectra for a trimer model with EET compared to experiment (black). Gray curves are the calculated exciton states. Frame B: Spectra calculated assuming no EET between monomers (blue) compared to experiment (black). The gray dashed curve is the calculated HB spectrum assuming no 60 cm^{-1} shift after burning. HB spectra are offset for clarity.

The importance of lifetime broadening (using the Redfield theory) was already demonstrated by modeling of HB spectra for various model dimers with weak el−ph coupling (S < 1).[42] Though for stronger el−ph coupling strength (S > 1), different line shape theories must be employed, as suggested in refs 43, 44, and 45, the Redfield approach is an appropriate approximation for systems with low el−ph coupling strength, i.e., for modeling various optical spectra of FMO complexes. In order to address the nature of the 825 nm band of FMO complexes, we applied a combination of Redfield and Förster theories to FMO complexes, simultaneously modeling absorption, emission, and nonresonant hole-burned spectra taking into account the uncorrelated EET between FMO monomers. That is, the exciton energies and lineshapes (including lifetime broadening) were modeled with Redfield theory as described previously,[42,46] while energy transfer rates between the lowest energy pigments of each monomer were calculated using the Förster theory.[34,35]

We used the spectral density for *C. tepidum* FMO from ref 47, which critically assessed the widely used spectral density functions. The above parameters were used in calculations of absorption, emission, and HB spectra, which are calculated for 50 000 complexes using a Monte Carlo approach, with site energies chosen randomly according to the SDF. A Huang−Rhys factor (S) of 0.4 was used and the effective S value (due to a small amount of delocalization) for the lowest excitonic state is 0.3, in agreement with previous ΔFLN data measured on the low-energy side of the 825 nm band.[25] The reorganization energy for the lowest energy state is about 12−14 cm^{-1}, in agreement with our experimental data,[48] and not 35 cm^{-1} as widely used in the theoretical calculations.[10,15,49,50] The monomer calculations in Figure 2 (frame B) cannot account for the positions of nonresonant holes or the emission spectrum, which is also too broad. The gray dashed curve in frame B is the calculated HB spectrum assuming no 60 cm^{-1} shift of the antihole (*vide infra*). While the hole positions are now more correct compared to experiment, the depth of the high-energy hole (~817 nm) is too large. Thus, the focus is placed on calculations assuming EET between monomer subunits, which explain the experimental optical spectra more convincingly. The calculated emission (frame A) is slightly red-

dx.doi.org/10.1021/jz5001165 | *J. Phys. Chem. Lett.* 2014, 5, 1450−1456

shifted due to the assumption that only the lowest state emits. However, the experimental emission spectrum could also possess a small contribution from a fraction of pigments contributing to sub-band 2, because for small coupling and, for example, EET on the order of 100 ps, sub-band 2 could also emit directly, albeit with reduced probability, even if sub-band 1 is not bleached.

The gray curves in frame A of Figure 2 represent the calculated excitonic states, with the three gray sub-bands of the 825 nm absorption band (curves 1−3) corresponding to sub-bands 1, 2, and 3, respectively. The peak positions of these sub-bands are 827.2, 825.6, and 823.8 nm. The calculated nonresonant HB spectrum, as expected, is a result of NPHB of the lowest energy state of FMO, whose shift results in redistribution of oscillator strength at various wavelengths. The agreement with experimental data suggests that BChl *a* 3 and 4 are indeed the main pigments contributing to the lowest energy exciton state, in agreement with refs 9−12. Modeling studies revealed that BChl *a* 5 and 7 do not contribute to the lowest energy band/hole, as these pigments have negligible excitonic interaction with BChl *a* 3. The best fit of the nonresonant hole in frame A was obtained assuming a 60 cm^{-1} blue-shift of postburn site energies; that is, after burning the site energy is shifted, on average, by 60 cm^{-1} to higher energy (see Figure 2).

Regarding the shape of the resonant HB spectra (see Figure 1), it is well-known[38,51] that the antihole (for low-dose HB spectra) is not uniformly distributed over the whole absorption band, rather it is typically distributed over the much narrower range both to the blue and to the red (by ∼10 cm^{-1}) of the ZPH, though larger blue-shifts are also observed.[38] The latter indicates the presence of different tiers in the protein energy landscape. For example, data shown in Figure 1 show that the antihole absorption is peaked at about 5−10 cm^{-1} to the blue and to the red of λ_B. Interestingly, the higher dose nonresonant HB spectrum shown in Figure 2 shows a larger average shift (∼60 cm^{-1}) of the antihole with respect to the main bleach. Similar behavior was observed for B800 BChl *a* molecules in the LH2 antenna complex of *Rhodopseudomonas acidophila*.[51] Thus, HB spectroscopy provides averaged magnitudes of light-induced spectral shifts, most likely probing two different tiers of the protein energy landscape. Similar ranges of spectral shifts were directly observed by a single photosynthetic complex study for B800 BChl *a* in *Rhodospirillum molischianum*.[52] The latter paper also discusses possible origins of various spectral shifts within the tiers of the potential energy hyper surface of a protein.

Figure 3 shows the contribution to the 825 nm absorption band (curve a) from pigments 3 (curve b) and 4 (curve c). Curves b′ and c′ illustrate their contribution to the nonresonant hole (curve a′). The sum of spectra b′ and c′ provides the calculated hole (red curve) shown in Figure 2 (frame A). The lowest energy excitonic state (with a maximum near 827.2 nm) has a relative oscillator strength of ∼0.86 BChl *a*, with largest contributions from BChl *a* 3 (80%). The delocalization length (inverse participation ratio) of the lowest excitonic state (sub-band 1) is 1.5. However, in our reduced structural trimer model, we have six excitonic states labeled as 1−6 in Figure 2A; thus, the oscillator strength for the remaining five exciton states in the BChl *a* 3/BChl *a* 4 trimer (i.e., three monomer subunits with the above-mentioned two pigments) are 0.81, 0.67, 1.40, 1.15, and 1.06. We hasten to add that excitons 4−6 (in our reduced FMO model) are mostly contributed to by BChl *a* 4 (∼80%) and BChl *a* 3 (∼20%), though in calculated spectra for

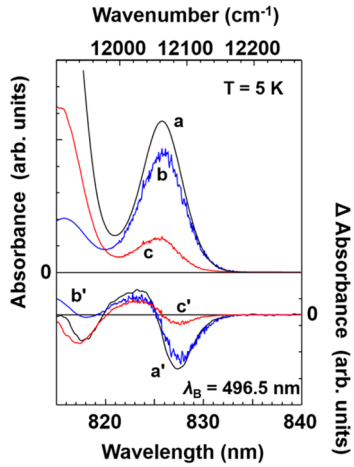

Figure 3. Spectra a and a′ (black curves) are the absorption and nonresonant HB spectra (λ_B = 496.5 nm). Spectra b/b′ and c/c′ represent the contributions from BChl *a* 3 and 4, respectively. The corresponding occupation numbers for BChl *a* 3 and 4 to the 825 nm absorption band are 80% and 20%, respectively.

the entire trimer the second exciton state is also in part contributed to by pigments 5 and 7 (to be reported elsewhere). Since only pigments 3 and 4 contribute to the 825 nm absorption band, our reduced structural model suffices to properly describe the 825 nm absorption, emission, and nonresonant HB spectra.

Figure 4 shows distributions of the relaxation times for sub-band 2 (frame A) and sub-band 3 (frame B) pigments,

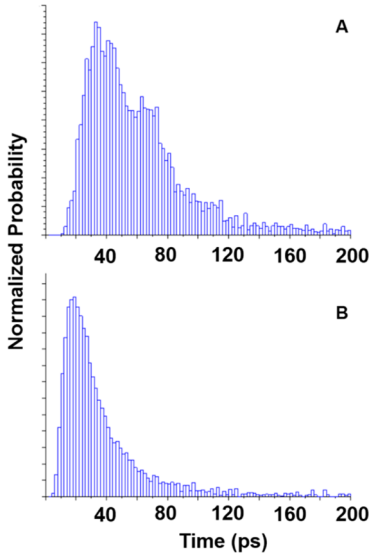

Figure 4. Distributions of Förster transfer times for pigments contributing to sub-band 2 (frame A) and sub-band 3 (frame B) obtained for V_{33} = −2.5 cm^{-1} (i.e., for the coupling between BChl *a* 3 pigments located in various monomers). The probabilities are normalized over 50 000 iterations (i.e., the sum of all probabilities is 1).

calculated with Förster theory for V_{33} = −2.5 cm^{-1}. The lowest energy pigment of each monomer is assumed to be BChl *a* 3. While the average relaxation time for sub-band 2 (positioned at 825.6 nm) is 70.0 ps, the distribution peaks at 32 ps. Likewise, the average and peak times for sub-band 3 are 41.3 and 20 ps, respectively. The average relaxation times assuming the lowest

dx.doi.org/10.1021/jz5001165 | J. Phys. Chem. Lett. 2014, 5, 1450−1456

energy pigment in one monomer of the trimer is BChl *a* 4 are 26.4 and 20.3 ps for sub-bands 2 and 3, respectively (data not shown). Recall that BChl *a* 4 contributes only 20% to the lowest energy band. It should be noted that in general Redfield theory predicts faster transfer rates (data not shown), as mentioned in ref 53. Previously reported experimental (high-resolution) resonant holes burned at λ_B = 822.8/824.8 nm (in *P. aestuarii*) and 823.0/825.0 nm (in *C. tepidum*) suggested the presence of downward energy transfer in the 825 nm absorption band.[24,54] In those papers, the observed average relaxation time of 37 ps, i.e., EET time obtained from λ_B = 823.0 nm, is in reasonable agreement with our finding (*vide supra*), in particular, when the distribution of EET times is taken into account. However, based on our data, it is difficult to estimate the average relaxation time for the middle of the 825 nm band (i.e., λ_B = 825.0 nm), as at this wavelength there are contributions from sub-bands 2 and 3, as well as the trap states that do not transfer energy (i.e., sub-band 1). The 37 ps component was also found in the kinetic measurements for FMO complexes (*P. aestuarii*) and was attributed to energy transfer between subunits of the FMO trimer,[30,55] in agreement with our data. The previously observed time-dependent red-shift of the FMO emission spectrum, where the ∼30 ps time constant was related to energy transfer in the protein trimer between monomer subunits[56] is also consistent with our model. Finally, studies focused on slower processes taking place in FMO complexes, both at room and 77 K temperatures, found that a complete spectral equilibration in FMO proteins occurs in about 26 ps,[29] which again is likely due to equilibration within the trimer caused by the uncorrelated EET discussed above.

In summary, as argued above, the HB spectra and modeling studies, along with previously reported data,[23−31] clearly indicate the existence of EET within the lowest absorption band of the FMO complex. Thus, in contrast to the presently accepted consensus[3,17] (suggesting that only one monomer can be used to describe linear optical spectra), we conclude that each trimer has three identical (degenerate) SDFs from the three monomers connected by Förster EET. Therefore, the 825 nm band in the FMO protein cannot be explained for by a single electronic transition. That is, for the very weak el−ph coupling observed ($S \sim 0.3$),[25] the broad and structured holes in Figure 1 cannot be explained by standard EET-free HB theory.[38] Also, the dependence of S across the 825 nm band observed in refs 25 and 26 is consistent with uncorrelated EET between monomers of the FMO trimer. Finally, our findings are also consistent with the shapes of the vibronically excited fluorescence line-narrowed spectra (data not shown for brevity), in which only very weak zero-phonon lines were superimposed on a broad fluorescence origin band, clearly supporting the EET within the FMO trimer.

We have demonstrated, using HB spectroscopy, that the 825 nm absorption band of the FMO trimer cannot be explained by a single electronic transition. To explain the shape of emission and nonresonant HB spectra, downward uncorrelated EET between trimer subunits should be taken into account. Of course uncorrelated EET between monomers is preceded by downward energy relaxation along the "excitonic energy ladder" in each monomer on a femtosecond time scale.[56,57] We propose that after light induced coherences vanish, uncorrelated EET between the lowest by exciton levels of each monomer takes place due to static structural inhomogeneity in the trimer leading to equilibration within the trimer that takes several tens of picoseconds.

AUTHOR INFORMATION

Corresponding Author

*E-mail: ryszard@ksu.edu.

Notes

The authors declare no competing financial interest.

ACKNOWLEDGMENTS

This work was supported by the Chemical Sciences, Geosciences and Biosciences Division, Office of Basic Energy Sciences, Office of Science, U.S. Department of Energy (Grant No. DE-FG02-11ER16281 to R.J.). We thank Dr. Robert E. Blankenship and Dr. Jianzhong Wen (Washington University in St. Louis) for providing the FMO samples and Mike Reppert (University of Chicago) for helpful discussions during the early stage of this project. We acknowledge Dr. Chen Lin for the measurements of vibronically excited fluorescence line-narrowed spectra. V.Z. acknowledges support of NSERC Discovery grant.

REFERENCES

(1) Olson, J. M.; Romano, C. A. A New Chlorophyll from Green Bacteria. *Biochim. Biophys. Acta* **1962**, *59*, 726−728.

(2) Olson, J. M. The FMO Protein. *Photosynth. Res.* **2004**, *80*, 181−187.

(3) Milder, M. T. W.; Brüggemann, B.; van Grondelle, R.; Herek, J. L. Revisiting the Optical Properties of the FMO Protein. *Photosynth. Res.* **2010**, *104*, 257−274.

(4) Engel, G. S.; Calhoun, T. R.; Read, E. L.; Ahn, T.-K.; Mančal, T.; Cheng, Y.-C.; Blankenship, R. E.; Fleming, G. R. Evidence for Wavelike Energy Transfer Through Quantum Coherence in Photosynthetic Systems. *Nature* **2007**, *446*, 782−786.

(5) Panitchayangkoon, G.; Hayes, D.; Fransted, K. A.; Caram, J. R.; Harel, E.; Wen, J.; Blankenship, R. E.; Engel, G. S. Direct Evidence of Quantum Transport in Photosynthetic Light-Harvesting Complexes. *Proc. Natl. Acad. Sci. U.S.A.* **2010**, *107*, 12766−12770.

(6) Ben-Shem, A.; Frolow, F.; Nelson, N. Evolution of Photosystem I − From Symmetry through Pseudosymmetry to Asymmetry. *FEBS Lett.* **2004**, *564*, 274−280.

(7) Tronrud, D. E.; Wen, J.; Gay, L.; Blankenship, R. E. The Structural Basis for the Difference in Absorbance Spectra for the FMO Antenna Protein from Various Green Sulfur Bacteria. *Photosynth. Res.* **2009**, *100*, 79−87.

(8) Wen, J.; Zhang, H.; Gross, M. L.; Blankenship, R. E. Native Electrospray Mass Spectrometry Reveals the Nature and Stoichiometry of Pigments in the FMO Photosynthetic Antenna Protein. *Biochemistry* **2011**, *50*, 3502−3511.

(9) Vulto, S. I. E.; de Baat, M. A.; Louwe, R. J. W.; Permentier, H. P.; Neef, T.; Miller, M.; van Amerongen, H.; Aartsma, T. J. Exciton Simulations of Optical Spectra of the FMO Complex from the Green Sulfur Bacterium *Chlorobium tepidum* at 6 K. *J. Phys. Chem. B* **1998**, *102*, 9577−9582.

(10) Vulto, S. I. E.; de Baat, M. A.; Louwe, R. J. W.; Permentier, H. P.; Neef, T.; Miller, M.; van Amerongen, H.; Aartsma, T. J. Exciton Simulations of Optical Spectra of the FMO Complex from the Green Sulfur Bacterium *Chlorobium tepidum* at 6 K. *J. Phys. Chem. B* **1998**, *102*, 9577−9582.

(11) Sarovar, M.; Cheng, Y.-C.; Whaley, K. B. Environmental Correlation Effects on Excitation Energy Transfer in Photosynthetic Light Harvesting. *Phys. Rev. E* **2011**, *83*, 011906.

(12) Vlaming, S. M.; Silbey, R. J. Correlated Intermolecular Coupling Fluctuations in Photosynthetic Complexes. *J. Chem. Phys.* **2012**, *136*, 055102.

(13) Schmidt am Busch, M.; Müh, F.; Madjet, M. E.-A.; Renger, T. The Eighth Bacteriochlorophyll Completes the Excitation Energy Funnel in the FMO Protein. *J. Phys. Chem. Lett.* **2011**, *2*, 93−98.
(14) Adolphs, J.; Renger, T. How Proteins Trigger Excitation Energy Transfer in the FMO Complex of Green Sulfur Bacteria. *Biophys. J.* **2006**, *91*, 2778−2797.
(15) Ishizaki, A.; Fleming, G. R. Theoretical Examination of Quantum Coherence in a Photosynthetic System at Physiological Temperature. *Proc. Natl. Acad. Sci. U.S.A.* **2009**, *106*, 17255−17260.
(16) Rebentrost, P.; Mohseni, M.; Aspuru-Guzik, A. Role of Quantum Coherence and Environmental Fluctuations in Chromophoric Energy Transport. *J. Phys. Chem. B* **2009**, *113*, 9942−9947.
(17) Caycedo-Soler, F.; Chin, A. W.; Almeida, J.; Huelga, S. F.; Plenio, M. B. The Nature of the Low Energy Band of the Fenna−Matthews−Olson Complex: Vibronic Signatures. *J. Chem. Phys.* **2012**, *136*, 155102.
(18) Huo, P.; Coker, D. F. Iterative Linearized Density Matrix Propagation for Modeling Coherent Excitation Energy Transfer in Photosynthetic Light Harvesting. *J. Chem. Phys.* **2010**, *133*, 184108.
(19) Wu, J.; Liu, F.; Shen, Y.; Cao, J.; Silbey, R. J. Efficient Energy Transfer in Light-Harvesting Systems, I: Optimal Temperature, Reorganization Energy and Spatial−Temporal Correlations. *New J. Phys.* **2010**, *12*, 105012.
(20) Wu, J.; Liu, F.; Ma, J.; Silbey, R. J.; Cao, J. Efficient Energy Transfer in Light-Harvesting Systems: Quantum-Classical Comparison, Flux Network, and Robustness Analysis. *J. Chem. Phys.* **2012**, *137*, 174111.
(21) Moix, J.; Wu, J.; Huo, P.; Coker, D.; Cao, J. Efficient Energy Transfer in Light-Harvesting Systems, III: The Influence of the Eighth Bacteriochlorophyll on the Dynamics and Efficiency in FMO. *J. Phys. Chem. Lett.* **2011**, *2*, 3045−3052.
(22) Mostame, S.; Rebentrost, P.; Eisfeld, A.; Kerman, A. J.; Tsomokos, D. I.; Aspuru-Guzik, A. Quantum Simulator of an Open Quantum System Using Superconducting Qubits: Exciton Transport in Photosynthetic Complexes. *New J. Phys.* **2012**, *14*, 105013.
(23) Johnson, S. G.; Small, G. J. Excited-State Structure and Energy-Transfer Dynamics of the Bacteriochlorophyll *a* Antenna Complex from *Prosthecochloris aestuarii*. *J. Phys. Chem.* **1991**, *95*, 471−479.
(24) Matsuzaki, S.; Zazubovich, V.; Rätsep, M.; Hayes, J. M.; Small, G. J. Energy Transfer Kinetics and Low Energy Vibrational Structure of the Three Lowest Energy Q_y-States of the Fenna−Matthews−Olson Antenna Complex. *J. Phys. Chem. B* **2000**, *104*, 9564−9572.
(25) Rätsep, M.; Freiberg, A. Electron−Phonon and Vibronic Couplings in the FMO Bacteriochlorophyll *a* Antenna Complex Studied by Difference Fluorescence Line Narrowing. *J. Lumin.* **2007**, *127*, 251−259.
(26) Rätsep, M.; Freiberg, A. Unusual Temperature Quenching of Bacteriochlorophyll *a* Fluorescence in FMO Antenna Protein Trimers. *Chem. Phys. Lett.* **2007**, *434*, 306−311.
(27) Savikhin, S.; Zhou, W.; Blankenship, R. E.; Struve, W. S. Femtosecond Energy Transfer and Spectral Equilibration in Bacteriochlorophyll *a*−Protein Antenna Trimers from the Green Bacterium *Chlorobium tepidum*. *Biophys. J.* **1994**, *66*, 110−114.
(28) Savikhin, S.; Struve, W. S. Ultrafast Energy Transfer in FMO Trimers from the Green Bacterium *Chlorobium tepidum*. *Biochemistry* **1994**, *33*, 11200−11208.
(29) Gulbinas, V.; Valkunas, L.; Kuciauskas, D.; Katilius, E.; Liuolia, V.; Zhou, W.; Blankenship, R. E. Singlet−Singlet Annihilation and Local Heating in FMO Complexes. *J. Phys. Chem.* **1996**, *100*, 17950−17956.
(30) Louwe, R. J. W.; Aartsma, T. J. On the Nature of Energy Transfer at Low Temperatures in the BChl *a* Pigment-Protein Complex of Green Sulfur Bacteria. *J. Phys. Chem. B* **1997**, *101*, 7221−7226.
(31) Louwe, R. J. W.; Vrieze, J.; Aartsma, T. J.; Hoff, A. J. Toward an Integral Interpretation of the Optical Steady-State Spectra of the FMO-Complex of *Prosthecochloris aestuarii*. 1. An Investigation with Linear-Dichroic Absorbance-Detected Magnetic Resonance. *J. Phys. Chem. B* **1997**, *101*, 11273−11279.
(32) Pearlstein, R. M. Theory of the Optical Spectra of the Bacteriochlorophyll *a* Antenna Protein Trimer from *Prosthecochloris aestuarii*. *Photosynth. Res.* **1992**, *31*, 213−226.
(33) Herascu, N.; Kell, A.; Acharya, K.; Jankowiak, R.; Blankenship, R. E.; Zazubovich, V. Modeling of Various Optical Spectra in the Presence of Slow Excitation Energy Transfer in Dimers and Trimers with Weak Inter-Pigment Coupling: FMO as an Example. *J. Phys. Chem. B* **2014**, *118*, 2032−2040.
(34) Förster, T. Zwischenmolekulare Energiewanderung und Fluoreszenz. *Ann. Phys. (Berlin)* **1948**, *437*, 55−75.
(35) Förster, T. Delocalized Excitation and Excitation Transfer. In *Action of Light and Organic Crystals*; Sinanoğlu, O., Ed.; Modern Quantum Chemistry: Istanbul Lectures, Part III; Academic: New York, 1965; pp 93−137.
(36) Madjet, M. E.; Abdurahman, A.; Renger, T. Intermolecular Coulomb Couplings from Ab Initio Electrostatic Potentials: Application to Optical Transitions of Strongly Coupled Pigments in Photosynthetic Antennae and Reaction Centers. *J. Phys. Chem. B* **2006**, *110*, 17268−17281.
(37) Hayes, J. M.; Ruehlaender, M.; Soukoulis, C.; Small, G. J. Monte Carlo Simulation of Energy Transfer Rates: Application to Downward Energy Transfer within the 825 nm Absorption Band of the FMO Complex of *Prosthecochloris aestuarii*. *J. Lumin.* **2002**, *98*, 249−255.
(38) Jankowiak, R.; Reppert, M.; Zazubovich, V.; Pieper, J.; Reinot, T. Site Selective and Single Complex Laser-Based Spectroscopies: A Window on Excited State Electronic Structure, Excitation Energy Transfer, and Electron−Phonon Coupling of Selected Photosynthetic Complexes. *Chem. Rev.* **2011**, *111*, 4546−4598.
(39) Jankowiak, R. Probing Electron-Transfer Times in Photosynthetic Reaction Centers by Hole-Burning Spectroscopy. *J. Phys. Chem. Lett.* **2012**, *3*, 1684−1694.
(40) Redfield, A. G. On the Theory of Relaxation Processes. *IBM J. Res. Dev.* **1957**, *1*, 19−31.
(41) Redfield, A. G. The Theory of Relaxation Processes. *Adv. Magn. Reson.* **1965**, *1*, 1−32.
(42) Reppert, M. Modeling of Resonant Hole-Burning Spectra in Excitonically Coupled Systems: The Effects of Energy-Transfer Broadening. *J. Phys. Chem. Lett.* **2011**, *2*, 2716−2721.
(43) Schröder, M.; Kleinekathöfer, U.; Schreiber, M. Calculation of Absorption Spectra for Light-Harvesting Systems Using Markovian Approaches as Well as Modified Redfield Theory. *J. Chem. Phys.* **2006**, *124*, 084903.
(44) Ishizaki, A.; Fleming, G. R. On the Adequacy of the Redfield Equation and Related Approaches to the Study of Quantum Dynamics in Electronic Energy Transfer. *J. Chem. Phys.* **2009**, *130*, 234110.
(45) Novoderezhkin, V. I.; van Grondelle, R. Physical Origins and Models of Energy Transfer in Photosynthetic Light-Harvesting. *Phys. Chem. Chem. Phys.* **2010**, *12*, 7352−7365.
(46) Renger, T.; Marcus, R. A. On the Relation of Protein Dynamics and Exciton Relaxation in Pigment−Protein Complexes: An Estimation of the Spectral Density and a Theory for the Calculation of Optical Spectra. *J. Chem. Phys.* **2002**, *116*, 9997−10019.
(47) Kell, A.; Feng, X.; Reppert, M.; Jankowiak, R. On the Shape of the Phonon Spectral Density in Photosynthetic Complexes. *J. Phys. Chem. B* **2013**, *117*, 7317−7323.
(48) Kell, A.; Acharya, K.; Blankenship, R. E.; Jankowiak, R. On Destabilization of the Fenna−Matthews−Olson Complex of *Chlorobaculum tepidum*. *Photosynth. Res.* **2014**, DOI: 10.1007/s11120.014-9900-y.
(49) Pachón, L. A.; Brumer, P. Physical Basis for Long-Lived Electronic Coherence in Photosynthetic Light-Harvesting Systems. *J. Phys. Chem. Lett.* **2011**, *2*, 2728−2732.
(50) Ritschel, G.; Roden, J.; Strunz, W. T.; Aspuru-Guzik, A.; Eisfeld, A. An Efficient Method to Calculate Excitation Energy Transfer in Light-Harvesting Systems: Application to the Fenna−Matthews−Olson Complex. *J. Phys. Chem. Lett.* **2011**, *2*, 2912−2917.
(51) Grozdanov, D.; Herascu, N.; Reinot, T.; Jankowiak, R.; Zazubovich, V. Low-Temperature Protein Dynamics of the B800 Molecules in the LH2 Light-Harvesting Complex: Spectral Hole

Burning Study and Comparison with Single Photosynthetic Complex Spectroscopy. *J. Phys. Chem. B* **2010**, *114*, 3426−3438.
(52) Hofmann, C.; Aartsma, T. J.; Michel, H.; Köhler, J. Direct Observation of Tiers in the Energy Landscape of a Chromoprotein: A Single-Molecule Study. *Proc. Natl. Acad. Sci. U.S.A.* **2003**, *100*, 15534−15538.
(53) Ishizaki, A.; Fleming, G. R. Unified Treatment of Quantum Coherent and Incoherent Hopping Dynamics in Electronic Energy Transfer: Reduced Hierarchy Equation Approach. *J. Chem. Phys.* **2009**, *130*, 234111.
(54) Rätsep, M.; Blankenship, R. E.; Small, G. J. Energy Transfer and Spectral Dynamics of the Three Lowest Energy Q_y-States of the Fenna-Matthews-Olson Antenna Complex. *J. Phys. Chem. B* **1999**, *103*, 5736−5741.
(55) Vulto, S. I. E.; Streltsov, A. M.; Aartsma, T. J. Excited State Energy Relaxation in the FMO Complexes of the Green Bacterium *Prosthecochloris aestuarii* at Low Temperatures. *J. Phys. Chem. B* **1997**, *101*, 4845−4850.
(56) Freiberg, A.; Lin, S.; Timpmann, K.; Blankenship, R. E. Exciton Dynamics in FMO Bacteriochlorophyll Protein at Low Temperatures. *J. Phys. Chem. B* **1997**, *101*, 7211−7220.
(57) van Amerongen, H.; Valkunas, L.; van Grondelle, R. *Photosynthetic Excitons*; World Scientific: Singapore, 2000.